BROOKHAVEN NATIONAL LABORATORY BNL--46322

June 1991 DE91 015833

STRANGE QUARKS IN NUCLEI

Carl B. Dover

Physics Department
Brookhaven National Laboratory
Upton, New York 11973

ABSTRACT

We survey the field of strange particle nuclear physics, starting with the spectroscopy of strangeness $S = -1$ Λ hypernuclei, proceeding to an interpretation of recent data on $S = -2$ $\Lambda\Lambda$ hypernuclear production and decay, and finishing with some speculations on the production of multi-strange nuclear composites (hypernuclei or "strangelets") in relativistic heavy ion collisions.

Invited talk presented at
the Intersections between Particle and Nuclear Physics
Tucson, Arizona
May 24–29, 1991

This manuscript has been authored under contract number DE-AC02-76CH00016 with the U.S. Department of Energy. Accordingly, the U.S. Government retains a non-exclusive, royalty-free license to publish or reproduce the published form of this contribution, or allow others to do so, for U.S. Government purposes.

STRANGE QUARKS IN NUCLEI

Carl B. DOVER

Brookhaven National Laboratory, Upton, New York 11973, USA

ABSTRACT

We survey the field of strange particle nuclear physics, starting with the spectroscopy of strangeness $S = -1$ Λ hypernuclei, proceeding to an interpretation of recent data on $S = -2$ $\Lambda\Lambda$ hypernuclear production and decay, and finishing with some speculations on the production of multi–strange nuclear composites (hypernuclei or "strangelets") in relativistic heavy ion collisions.

1. INTRODUCTION

In this talk, we explore the strangeness (S) degree of freedom in nuclei. We start with a discussion of $S = -1$ hypernuclei, which consist of a single hyperon (Λ or Σ) embedded in the nuclear medium. Recent (π^+, K^+) data from Brookhaven have revealed the single particle states of the Λ as a function of mass number A. These are interpreted in terms of a Λ–nucleus mean field theory, yielding the Λ–nucleus well depth, spin–orbit potential, and effective mass. Prospects for qualitative advances in hypernuclear spectroscopy depend on the possibility of performing experiments with good energy resolution ($\Delta E < 0.5$ MeV). We discuss the motivation for such experiments by means of selected examples: such a program could be implemented with electron beams at CEBAF or at a future pion linear accelerator (PILAC).

There has been some recent progress in identifying candidates for $S = -2$ hypernuclei in a hybrid counter–emulsion experiment at KEK. We discuss a consistent dynamical interpretation of this data, and suggest some key experiments, involving neutron or γ emission from Ξ^- atoms, which would augment our slender body of knowledge of the properties of $\Lambda\Lambda$ hypernuclei.

Finally, we consider the possibilities for producing and exploring the properties of multi–strange ($S \leq -3$) nuclear systems, either weakly bound multi–Λ hypernuclei with conventional weak decay lifetimes, or more strongly bound "strangelets", quark droplets which could even be stable with respect to weak neutron emission. Relativistic heavy ion collisions provide the best prospects for producing multi–strange clusters. We provide some rough estimates of the rates for strange cluster formation in central Au+Au collisions, and describe an experiment to be carried out at the Brookhaven AGS, which will search for such objects with a sensitivity approaching 10^{-11} per collision.

This work was supported by the Department of Energy under Contract No. DE-AC02-76CH00016

2. Λ SINGLE PARTICLE STRUCTURE

The principal production mechanisms for Λ hypernuclei have been strangeness exchange ($K^- + n \rightarrow \pi^- + \Lambda$) and associated production ($\pi^+ + n \rightarrow K^+ + \Lambda$). The (K^-, π^-) at forward angles corresponds to a small momentum transfer q, while the (π^+, K^+) reaction is characterized by $q \geq 300$ MeV/c. Thus the (K^-, π^-) process excites predominantly non–spin–flip transitions with low orbital angular momentum transfer ΔL, while (π^+, K^+) tends to emphasize non–spin–flip transitions of maximum ΔL. The (γ, K^+) photoproduction reaction is kinematically similar to (π^+, K^+), but strongly favors spin–flip transitions. These features are treated in detail in several review articles[1–3].

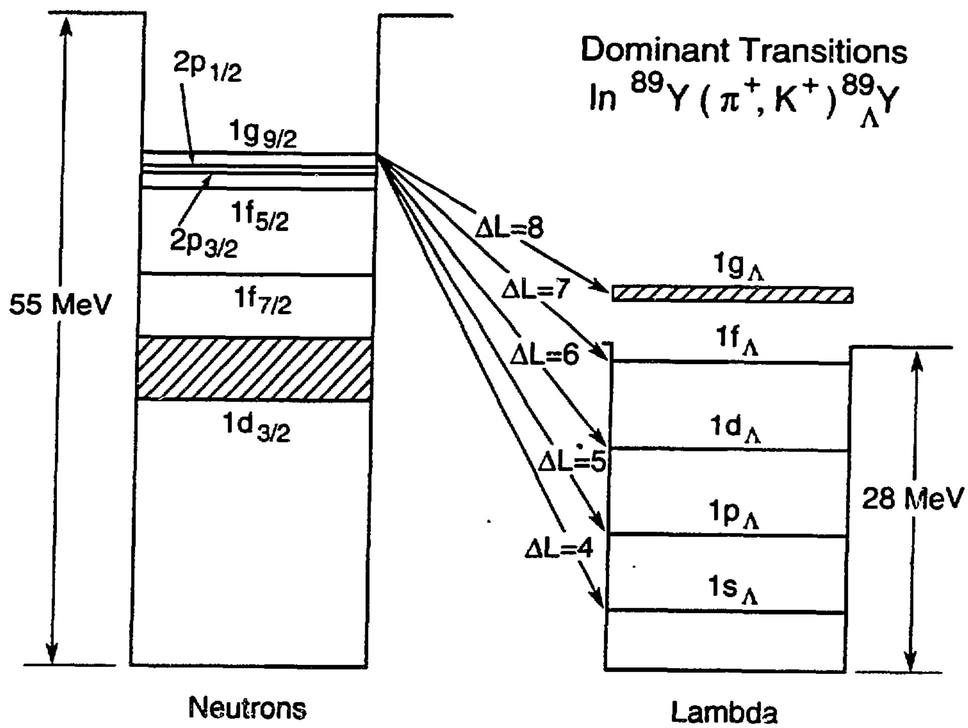

Figure 1: Single particle states in a neutron potential well (left side, for $N = 50$) or a Λ well (right side). The arrows indicate the major transitions of maximum ΔL induced by the (π^+, K^+) reaction.

The dominant single particle transitions induced by the (π^+, K^+) reaction on a nucleus with neutron number $N = 50$ (ex. ^{89}Y) are shown in Fig. 1. The (π^+, K^+) cross sections at $\theta = 10^\circ$ have been measured[3] at the Brookhaven AGS for seven nuclear targets from ^{9}Be to ^{89}Y. A sample of this data, for the reaction $^{89}\mathrm{Y}(\pi^+, K^+)^{89}_{\Lambda}\mathrm{Y}$, is displayed in Fig. 2. In spite of the coarse energy resolution of $\Delta E \approx 3$ MeV, a series of well defined peaks is visible in the data. These can be attributed[4] to single particle transitions from various neutron shell model orbits

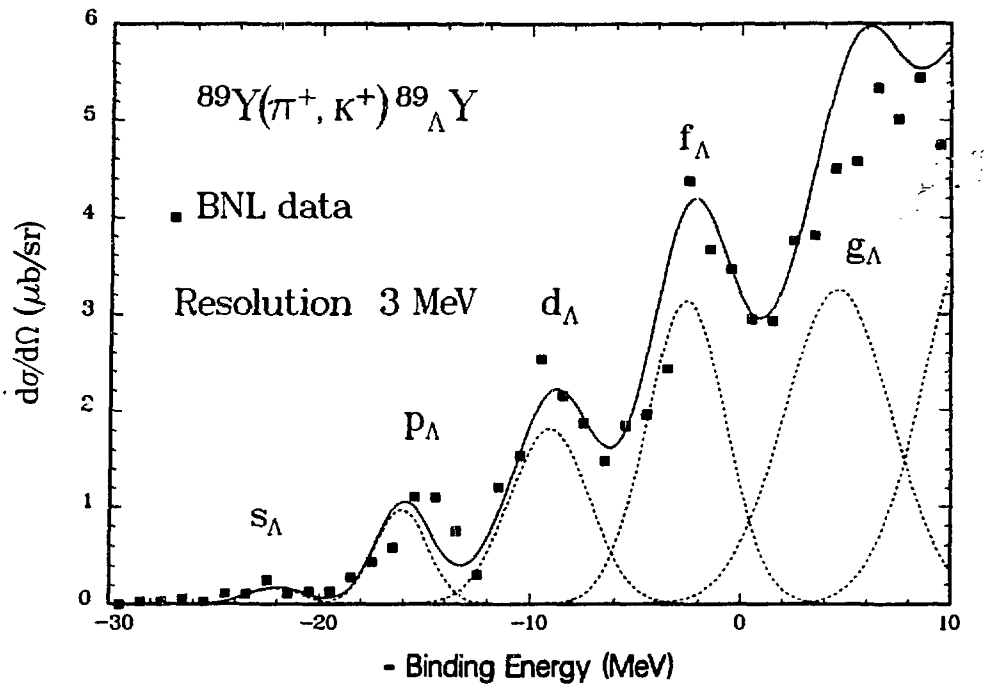

Figure 2: The excitation spectrum for the $^{89}Y(\pi^+, K^+)^{89}_{\Lambda}Y$ reaction at 1.05 GeV/c and $\theta = 10°$, from a Brookhaven AGS experiment[3]. The curves represent DWBA calculations (multiplied by an overall factor of 0.71) using a Fermi-averaged $\pi^+ n \to K^+ \Lambda$ amplitude, optical potentials fit to π^+ and K^+ elastic scattering at 800 MeV/c, Woods–Saxon bound state potentials, and the experimental distribution of neutron pickup strength from ^{90}Zr. The $(\ell_\Lambda \otimes g_{9/2}^{-1})$ contributions are indicated by dashed curves.

$\{\ell_n, j_n\}$ to Λ orbits $\{\ell_\Lambda, j_\Lambda\}$. The solid line in Fig. 2 represents the results of a reaction calculation[5] in distorted wave Born approximation (DWBA), while the dashed line shows the dominant contributions to the peaks arising from high-spin couplings of $(\ell_\Lambda \otimes g_{9/2}^{-1})$ configurations. The high spin of the last-filled $g_{9/2}$ orbit in ^{89}Y provides many neutrons (10 in the simple shell model limit) on which $n \to \Lambda$ conversion can take place, and enables the preference for large ΔL and q to be satisfied. The DWBA calculation is seen to give a semi-quantitative account of the absolute (π^+, K^+) cross section and its dependence on excitation energy.

An analysis of all the (π^+, K^+) data, similar to that depicted in Fig. 2, enables us to extract s_Λ, p_Λ, d_Λ and f_Λ single particle energies as a function of mass number A. Because of the coarse resolution $\Delta E = 3$ MeV, we are not able to resolve any spin splittings. The Λ-nucleus spin–orbit potential, for instance, is known to be small[6], and splittings due to spin–spin and tensor ΛN forces[7] are also very modest. Thus each peak in Fig. 2 represents a sum over a number of unresolved states. Basically, the (π^+, K^+), as well as earlier (K^-, π^-) data provide us with the spacing of Λ quasi-particle levels of different orbital angular momentum ℓ_Λ.

The spacings of the Λ levels for a given A constrain both the radius and the depth of the Λ–nucleus potential well. The data on Λ single particle states can be quantitatively reproduced[8] by a Skyrme–Hartree–Fock mean field approach, familiar from many similar analyses of nucleon levels. In this model, the equivalent energy dependent local potential $V_\Lambda(r, E)$ for the Λ is of the form

$$\begin{aligned}
V_\Lambda(r,E) &= \frac{m^*_\Lambda(r)}{m_\Lambda} U(r) + \left(1 - \frac{m^*_\Lambda(r)}{m_\Lambda}\right) E \\
U(r) &= t_0 \rho(r) + \frac{3}{8} t_3 \rho^2(r) + \frac{1}{4}(t_1 + t_2) T(r) \\
T(r) &= \frac{3}{5}\left(\frac{3\pi^2}{2}\right)^{2/3} \rho^{5/3}(r) \\
\frac{\hbar^2}{2m^*_\Lambda(r)} &= \frac{\hbar^2}{2m_\Lambda} + \frac{1}{4}(t_1 + t_2)\rho(r)
\end{aligned} \tag{1}$$

where $\rho(r)$ is the nuclear density. Here, the non–locality of the Λ–nucleus mean field is parametrized in terms of an effective mass $m^*_\Lambda(r)$. The parameters t_i are adjusted to fit the data: Millener *et al.*[8] obtain $t_0 \approx -400$ MeV $\cdot$ fm^3, $t_1 + t_2 \approx 100$ MeV $\cdot$ fm^5 and $t_3 \approx 3400$ MeV $\cdot$ fm^6. The term linear in $\rho(r)$ corresponds to a depth $t_0\rho_0 \approx -65$ MeV, consistent with estimates based on the free space ΛN interaction[9]. The repulsive term $t_3\rho^2(r)$ can be used to adjust the radius of the potential, while the term dependent on the energy E serves to spread out the single particle levels, enabling one to simultaneously fit the spectra of light and heavy hypernuclei. The resulting Λ well depth is 28 MeV, about 1/2 of the neutron well depth. The radius of the Λ potential is about 0.5 fm larger than that of $\rho(r)$, due to the non–linear terms in the density.

A single choice of parameters in the mean field picture (Eq. (1)) leads to a successful description of both loosely and deeply bound Λ orbitals, in contrast to the situation for nucleon orbitals[10]. Unlike deeply bound nucleon–hole states, known from $(e, e'p)$ studies to be very broad, Λ quasiparticle states remain well defined, even deep inside the nucleus.

3. PROSPECTS FOR HIGH RESOLUTION STUDIES

Coarse resolution experiments have enabled us to deduce the single particle properties of Λ's in nuclei. In addition, some properties of the ΛN residual interaction have been extracted from detailed analysis[11] of individual hypernuclear spectra, for instance ${}^{13}_{\Lambda}$C. From the limited data on electromagnetic transitions in hypernuclei, from $(K^-, \pi^-\gamma)$ studies[12], we have obtained some constraints on the spin dependence of the ΛN interaction[7], but the available information is incomplete.

To make qualitative progress in hypernuclear structure physics, we need to resolve the fine structure splittings, and this requires high resolution facilities. Hypernuclear spin splittings are small ($\leq$ 500 keV), so an energy resolution of order $\Delta E \approx 200$ keV is highly desirable. With the advent of the continuous beam (CW) electron accelerator CEBAF, it becomes feasible to perform hypernuclear experiments with real $[(\gamma, K)]$ or virtual $[(e, e'K)]$ photons. Another extremely promising alternative would be afforded by very intense pion beams in the 1 GeV/c region, for instance from PILAC, the pion linear accelerator[13] being discussed for construction at LAMPF. We discuss these possibilities in turn.

The $(\overline{K}, \pi)$ and (π, K) reactions on spin zero targets excite only non–spin–flip natural parity $(0^+, 1^-, 2^+$, etc.) states at 0°. The (γ, K) process, on the other hand, preferentially excites unnatural parity states, and is thus complementary to the hadronic reactions. The leading momentum–independent part of the $\gamma N \rightarrow K\Lambda$ transition operator is proportional to $\vec{\sigma} \cdot \hat{\epsilon}$, where $\vec{\sigma}$ and $\hat{\epsilon}$ are the nucleon spin and photon polarization, respectively. This term dominates for transitions to particle–hole configurations $(j_N^{-1} j_\Lambda)J$, for nodeless $j = \ell + 1/2$ orbits with maximum $J = \ell_N + \ell_\Lambda + 1$. For weaker transitions, configuration mixing as well as the momentum dependent terms in the (γ, K) operator are likely to be significant.

Results of particle–hole calculations[14] for the reaction ${}^{12}\mathrm{C}(\gamma, K^+){}^{12}_{\Lambda}\mathrm{B}^*$ are shown in Fig. 3. Contributions from the $(s^{\Lambda}_{1/2}\, p^{-1}_{3/2})$, $(p^{\Lambda}_{1/2,3/2}\, p^{-1}_{3/2})$, $(s^{\Lambda}_{1/2}\, s^{-1}_{1/2})$ and $(p^{\Lambda}_{1/2,3/2}\, s^{-1}_{1/2})$ configurations are included. The largest (γ, K^+) cross section corresponds to the highest spin $(p^{\Lambda}_{3/2}\, p^{-1}_{3/2})_{3^+}$ state, which is excited with negligible strength in the (π^+, K^+) or (K^-, π^-) reaction on ^{12}C. The strengths of the two components of the ground state doublet $(s^{\Lambda}_{1/2}\, p^{-1}_{3/2})_{1^-,2^-}$ are seen to be comparable, and hence one may be able to measure their splitting directly in a high resolution (γ, K) experiment. Except for the measured 1.1 MeV splitting[15] of the $(s^{\Lambda}_{1/2}\, s^{-1}_{1/2})_{0^+,1^+}$ configurations in ${}^{4}_{\Lambda}$He and ${}^{4}_{\Lambda}$H, no other doublet splittings are known.

As another example of a case where one could use the (γ, K^+) or $(e, e'K^+)$ reaction with good resolution to resolve the members of an s_Λ doublet, we consider the ${}^{9}\mathrm{Be}(\gamma, K^+){}^{9}_{\Lambda}\mathrm{Li}$ reaction. The ΛN interaction used to estimate these splittings is of the form

$$\begin{aligned} V_{\Lambda N}(r) =& V_0(r) + V_\sigma(r)\,\vec{\sigma}_N \cdot \vec{\sigma}_\Lambda + V_\Lambda(r)\,\vec{\ell}_{N\Lambda} \cdot \vec{\sigma}_\Lambda \\ &+ V_N(r)\,\vec{\ell}_{N\Lambda} \cdot \vec{\sigma}_N + V_T(r)\,S_{12} \end{aligned} \quad (2)$$

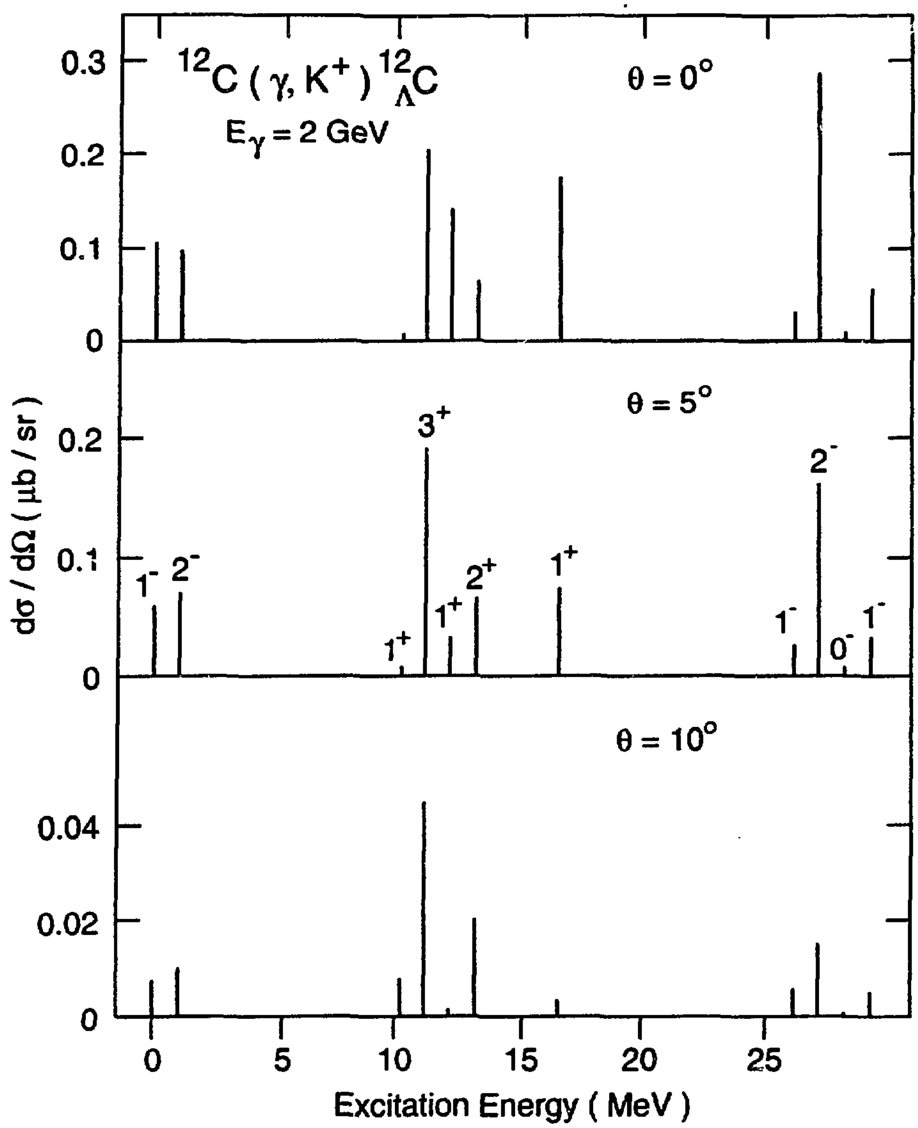

Figure 3: Predicted differential cross sections for the reaction $^{12}C(\gamma, K^{+})^{12}_{\Lambda}B^{*}$ at 2 GeV and various kaon angles θ_K. Note the dominance of spin–flip transitions to unnatural parity $(2^{-}, 3^{+})$ particle–hole states.

The relevant $p_N\, s_\Lambda$ interaction can be expressed in terms of five radial integrals $\overline{V}$, Δ, S_Λ, S_N and T, assumed to be constant across the p–shell and corresponding to the five terms in Eq. (2), respectively. The doublet splittings $\Delta E(s^{\Lambda}_{1/2})$ are predicted[2] to be

$$\Delta E\left(s^{\Lambda}_{1/2}\right) = \begin{cases} 1.21\Delta + 1.21 S_\Lambda + 1.00T & \left(s^{\Lambda}_{1/2} \otimes 2^{+}\right) \\ 0.69\Delta + 0.73 S_\Lambda - 3.3T & \left(s^{\Lambda}_{1/2} \otimes 1^{+}\right) \end{cases} \tag{3}$$

The largest contribution to ΔE arises from Δ, i.e., the $\vec{\sigma}_N \cdot \vec{\sigma}_\Lambda$ interaction. The splitting $\Delta E \approx 0.5$ MeV of the ground state ${}^9_\Lambda$Li doublet should be measurable at CEBAF. Many other s_Λ doublet splittings are probably too small to be measured directly, even with a resolution $\Delta E = 200$ keV. In most cases, however, unresolved peaks due to doublets based on different nuclear core states should be well separated: there is information on $V_{\Lambda N}$ to be gained from the energy separation of such peaks and the magnitude of the cross sections as a function of energy and momentum transfer.

The proposed pion linear accelerator (PILAC) at LAMPF offers the exciting prospect of high resolution (π^+, K^+) reaction studies[13], a necessary complement to the (γ, K) experiments at CEBAF. PILAC would employ high–gradient superconducting cavities to accelerate pions from LAMPF to the vicinity of 1 GeV/c, providing 10^9 π^+/sec on target and 200 keV resolution. This facility would generate an unprecedented intensity of pions at a momentum near the peak of the $\pi^+ n \rightarrow K^+ \Lambda$ cross section. The physics motivation for PILAC is rather broad, and was developed in detail in a recent Workshop[13]. In addition to the (π^+, K^+) studies emphasized here, we also mention the possibilities for detailed investigations of the structure and decays of N^* and Δ^* resonances, and the study of the interactions and decays of η mesons (a tagged η beam can be produced via the $\pi^- p \rightarrow \eta n$ process).

As an example of the capabilities of PILAC for hypernuclear structure studies, consider the ^{12}C$(\pi^+, K^+){}^{12}_\Lambda$C reaction. Three core states of ^{11}C, with large neutron spectroscopic factors, are important. Coupling an s_Λ or p_Λ to these core states produces a rich spectrum of states, a subset of which can be seen with the (π^+, K^+) reaction. In the top half of Fig. 4, we show the cross section[3] measured at Brookhaven with $\Delta E = 3$ MeV, together with the results of DWBA calculations[5]. The strength of the two smaller 1^- states cannot be extracted from this data. At the bottom of Fig. 4, we display the predicted[5] spectrum for a ^{12}C$(\pi^+, K^+){}^{12}_\Lambda$C experiment at PILAC. The difference between the top and bottom spectra in Fig. 4 is like night and day! The energy splittings and relative strengths of the three 1^- states, for instance, are very sensitive to the configuration mixing induced by $V_{\Lambda N}$. Only a high resolution spectrum can reveal the subtle action of the ΛN residual interaction at a level commensurate with our detailed knowledge of the NN interaction.

4. $S = -2$ HYPERNUCLEI

For hadronic systems containing two strange quarks, new possibilities arise. One anticipates the existence of a large array of conventional double hypernuclei ($S = -2$), containing two Λ hyperons in bound states, and possibly some quasiparticle Ξ–nucleus configurations[16], where the strong decay width due to $\Xi N \rightarrow \Lambda\Lambda$ conversion is not too large. At the quark level, there exists the possibility of more deeply bound multi–strange states, for instance the six quark H dibaryon[17](a $(ssuudd)$ composite with $J = I = 0$) or "strangelets" of larger baryon number and strangeness[18]. There exist other predictions of multistrange

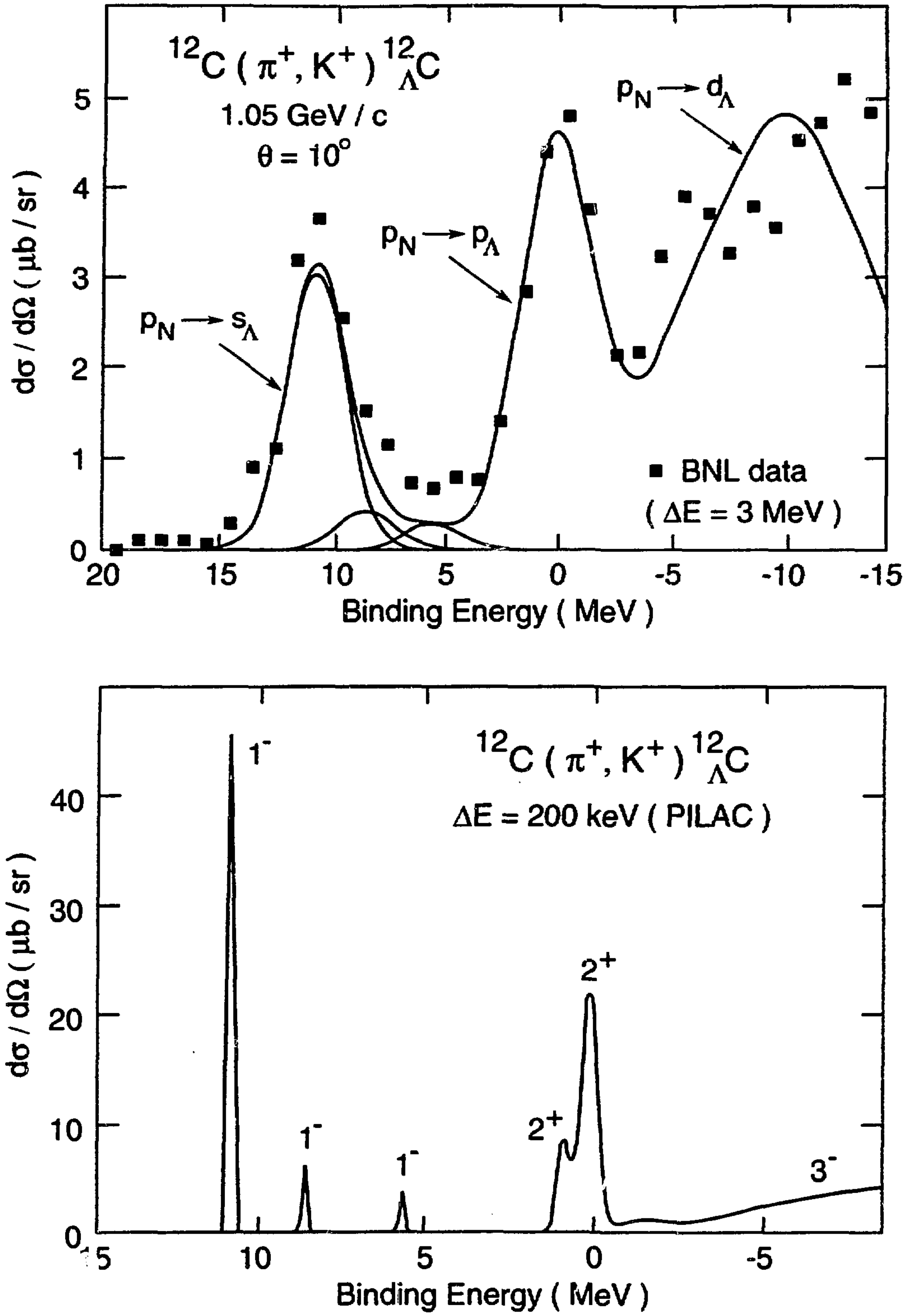

Figure 4: The excitation spectrum for the $^{12}C(\pi^+, K^+)^{12}_{\Lambda}C$ reaction at 1.05 GeV/c and $\theta = 10°$. In the top half, the measured Brookhaven data[3] with energy resolution $\Delta E = 3$ MeV are compared with the results of a DWBA calculation[5]. At the bottom, the predicted spectrum with $\Delta E = 200$ keV is shown. This resolution is attainable at PILAC.

dibaryon states, for instance in a version of the SU(3) soliton model[19], where $\Sigma^-\Sigma^-$, $\Xi\Xi$ and even $\Omega^-\Omega^-$ bound states are anticipated. These very speculative suggestions have led to a rekindling of interest in the properties of $\Lambda\Lambda$ hypernuclei, since if these are observed to decay by ordinary weak interactions, one could rule out the existence of the H dibaryon in a certain mass region. That is, unless the H hides close to the $\Lambda\Lambda$ threshold, one should observe strong decay (ex. ${}^{6}_{\Lambda\Lambda}\text{He} \to H + {}^{4}\text{He}$) rather than weak decay. The study of $\Lambda\Lambda$ hypernuclear spectra is also of interest in its own right, since one can explore the SU(3) structure of the baryon–baryon strong interactions, for instance by comparing the ${}^1\text{S}_0$ $\Lambda\Lambda$ and nn interactions, This sheds light on the nature of SU(3) symmetry breaking[20] of the strong forces of QCD.

In early emulsion experiments with K^- beams, evidence for the existence of ${}^{6}_{\Lambda\Lambda}\text{He}$ and ${}^{10}_{\Lambda\Lambda}\text{Be}$ was reported[21]; the soundness of the ${}^{10}_{\Lambda\Lambda}\text{Be}$ interpretation was reaffirmed by Dalitz *et al.*[22]. Recently, new experiments have been done at the KEK facility in Japan with a 1.66 GeV/c K^- beam[23]. A K^+ was detected to tag the formation of a Ξ^- via the $K^-p \to K^+\Xi^-$ reaction, and the Ξ^- was slowed down and captured at rest in emulsion. The resulting $\Xi^-p \to \Lambda\Lambda$ process can then produce states of single or double hypernuclei. An event was seen by Aoki *et al.*[23] which is kinematically consistent with the formation of ${}^{10}_{\Lambda\Lambda}\text{Be}$ or ${}^{13}_{\Lambda\Lambda}\text{B}$. The ${}^{13}_{\Lambda\Lambda}\text{B}$ interpretation, pointed out by Dover *et al.*[24], is consistent with the following reaction chain:

$$\Xi^- + {}^{14}\text{N} \to n + {}^{14}_{\Lambda\Lambda}\text{C}^* \to n + p + {}^{13}_{\Lambda\Lambda}\text{B} \qquad (4a)$$

$${}^{13}_{\Lambda\Lambda}\text{B} \to \pi^- + {}^{13}_{\Lambda}\text{C} \qquad (4b)$$

$${}^{13}_{\Lambda}\text{C} \to 2n + {}^{3}\text{He} + {}^{4}\text{He} + {}^{4}\text{He} \qquad (4c)$$

Eq. (4a) corresponds to a sequence of two–body decays, proceeding through a relatively long–lived excited state

$${}^{14}_{\Lambda\Lambda}\text{C}^* \approx (1s)_\Lambda\,(1p)_\Lambda \otimes {}^{12}\text{C}^*\,(T=1) \qquad (5)$$

at about 24 MeV of excitation. Here ${}^{12}\text{C}^*$ is an isovector core state (the 1^+ at 15.1 MeV or the 2^+ at 16.1 MeV). This *attractive* $\Lambda\Lambda$ interaction energy $\Delta B_{\Lambda\Lambda} = 4.8 \pm 0.7$ MeV (an $(s_\Lambda)^2$ matrix element) is consistent with earlier results[21] from ${}^{6}_{\Lambda\Lambda}\text{He}$ and ${}^{10}_{\Lambda\Lambda}\text{Be}$. For comparison, we note that the corresponding ${}^1\text{S}_0$ $(s_N)^2$ matrix element is 5–8 MeV, while the $(s_\Lambda\, s_N)$ ΛN matrix element (from the ${}^{5}_{\Lambda}\text{He}$ binding energy) is 2–3 MeV. Thus the $\Lambda\Lambda\,({}^1\text{S}_0)$ interaction seems to be more attractive than that for $\Lambda N\,({}^1\text{S}_0)$, and comparable to $NN\,({}^1\text{S}_0)$.

The relatively large value of $\Delta B_{\Lambda\Lambda}$ poses an interesting theoretical problem. The ${}^1\text{S}_0$, $S=-2$ dibaryon interaction presents a rather special situation in the quark model, because of the possibility of a bound state, the H. In the SU(3) limit, the H corresponds to the unitary singlet combination of $\Lambda\Lambda$, $\Sigma\Sigma$, and ΞN channels at short distances. In the meson exchange picture, the ${}^1\text{S}_0$ $(\Lambda\Lambda \to \Lambda\Lambda)$ interaction is attractive[24], and we do not expect strong short distance repulsion due to quark–gluon exchange, due to the strong channel coupling[25]. Thus $\Delta B_{\Lambda\Lambda} > 0$, corresponding to attraction, is expected in any reasonable model.

There are other interesting prospects for studying $\Lambda\Lambda$ hypernuclei, without relying on the observation of weak decays, as in Eqs. (4b, 4c). Zhu *et al.*[26] have estimated a branching ratio of order 3% for the reaction

$$\Xi^- + {}^6\mathrm{Li} \rightarrow {}^{6}_{\Lambda\Lambda}\mathrm{He} + n \tag{6}$$

This process is amenable to study, with the beam intensities available at the new high momentum K^- line at the Brookhaven AGS, currently being used for two H dibaryon searches[27,28] via the reactions

$$\Xi^- + d \rightarrow H + n \tag{7a}$$

$$K^- + {}^3\mathrm{He} \rightarrow K^+ + H + n \tag{7b}$$

For heavier p-shell targets, the $(1s_\Lambda)^2$ ground state yields in the $\Xi^- + {}^A\mathrm{Z} \rightarrow {}^{A}_{\Lambda\Lambda}(\mathrm{Z}-1) + n$ reaction are suppressed[26], and states of structure $(1s_\Lambda\, 1p_\Lambda)$, coupled to an excited core, are more strongly populated. Eqs. (4a) and (5) provide an example of this selectivity. Experimentally, one could also look for $E1$ γ rays emitted from excited $\Lambda\Lambda$ hypernuclear states; some examples are given by Zhu *et al.*[26].

More experimental data on $S = -2$ hypernuclei are required before we can quantitatively explore a number of interesting questions, such as the spin dependence of the $\Lambda\Lambda$ interaction, the breaking of SU(3) symmetry, and the implications for the existence of the H. Experiments with 1.5 – 2 GeV/c K^- beams at the AGS and KEK should be energetically pursued.

5. MULTIPLY STRANGE COMPOSITE OBJECTS

If we start with an ordinary nucleus, say ^{208}Pb, and start replacing neutrons by Λ hyperons, we can add many units of strangeness before the system becomes unstable with respect to strong decay[29]. These multi–Λ systems would have binding energies per particle B/A of a few MeV, and decay weakly with lifetimes of the order of 0.2 ns, due mostly to the non–mesonic process $\Lambda N \rightarrow NN$. There may also exist systems[18], called "strangelets", which have $|S| \approx A$, but possess a much larger B/A than an assembly of Λ's. For sufficiently large A, depending on the choice of bag pressure and quark–gluon coupling constant, these objects could be stable with respect to both strong and weak nucleon emission. In a "strangelet", a strange s quark is not necessarily correlated with a $(ud)_{I=0}$ pair to form a Λ; the s quarks are confined in the volume of the strangelet as a whole, but not within an individual Λ.

Berger and Jaffe[30] have provided a strangelet binding energy formula of Bethe–Weizäcker type:

$$B(A,Y,Z)/A = a_V - a_S/A^{1/3} - \left(\frac{a_C}{A^{4/3}} + \frac{\delta_Z}{2A^2}\right)(Z - Z_{\mathrm{min}})^2$$

$$-\frac{1}{2}\frac{\delta_Y}{A^2}(Y - Y_{\mathrm{min}})^2 \tag{8}$$

In addition to volume (a_V), surface (a_S) and Coulomb (a_C) terms which also occur in the usual nuclear mass formula[31], Eq (8) contains a term dependent on the hypercharge Y. For ordinary nuclei, we have $a_V = 15.5$ MeV, the binding energy per particle of infinite nuclear matter. Eq. (8) can be used to explore the regions of stability[30] against strong and weak neutron decay. For $Y = Y_{\rm min}$, $Z = Z_{\rm min}$, the intersection point of the strong and weak decay regions corresponds to $A = A_{\rm min}$, where[32]

$$A_{\rm min}^{1/3} = \frac{2a_S}{3a_V} \approx \frac{60 \text{ MeV}}{a_V} \tag{9}$$

The value $A_{\rm min}$ is significant for experiments, since it represents the lightest object with $Y = Y_{\rm min}$ which is likely to be long–lived (lifetime $\tau \gg \tau_\Lambda \approx 0.3$ ns). Strangelet searches may be viewed as placing a constraint on a_V. Based on later estimates of production rates (see Fig. 5) it is likely that $a_V \geq 30$ MeV is required if these objects are to be observable in high energy heavy ion collisions.

The only practical way of producing multi–strange hypernuclei or strangelets in the laboratory is by means of relativistic heavy ion collisions. In an encounter between heavy ions, each of the independent nucleon–nucleon collisions is capable of producing an $s\bar{s}$ quark pair. It is already known from AGS experiments at 15 GeV/A that substantial numbers of strange particles are produced in heavy ion central collisions[33]. Searches of modest sensitivity for long–lived strangelets have already been performed[34], with negative results. However, to obtain a meaningful test for the existence of strangelets, very high sensitivity measurements are required. This is the goal of experiment E864 at Brookhaven[35], which can attain sensitivities ϵ in the range 10^{-10} to 10^{-11} per collision for the detection of a variety of long–lived ($\tau > 5 - 10$ ns) objects of either positive or negative charge. These include anti–nuclei ($\bar{d}$, $\bar{t}$) and unusual nuclei (^{8}He, etc.) as well as strangelets. The production of $\bar{d}$'s has been seen at a very low rate in experiment E858 at Brookhaven[36]; clearly very high sensitivity will be required to detect $\bar{t}$'s.

There are no quantitative estimates of strangelet production rates in heavy ion collisions, but there are some interesting conjectures on the distillation of strange matter in the hadronization of quark–gluon–plasma[37]. To set the scale, it is perhaps useful to provide estimates for the formation of multi–strange objects via a conventional hadronic coalescence mechanism[38]. This is a conservative approach which neglects other production processes in dense matter which may occur at an earlier stage of the collision, before freezeout. For non–strange nuclei, the coalescence picture is well established[39] at BEVALAC energies (0.4–2 GeV/A). We write the number of clusters $N(A,S)$ of baryon number A and strangeness S produced per collision as

$$N(A,S) = \frac{N(A,S)}{N(A,0)} \frac{N(A,0)}{N_\alpha} N_\alpha \tag{10}$$

In the coalescence picture, the addition of one unit of baryon number ($S = 0$) to a cluster corresponds to a penalty factor P, while the conversion of a non–strange quark u, d to a strange quark s at fixed A leads to a strangeness suppression factor λ. Thus we have

$$\frac{N(A,S)}{N(A,0)} \approx \lambda^{|S|} \quad ; \quad \frac{N(A,0)}{N_\alpha} \approx P^{A-4} \tag{11}$$

In the thermal model[40], we have

$$P \approx \rho_p \lambda_T^3 \quad ; \quad \lambda_T = h/(2\pi m_p T)^{1/2} \tag{12}$$

where ρ_p is the proton density at freezeout, λ_T is the thermal wavelength, and T is the temperature. From the t/p and α/p ratios[39] measured in 2 GeV/A collisions at the BEVALAC, we obtain $P \approx 0.2$. For the higher energy AGS collisions, T is larger, and we estimate $P \approx 0.1$ from Eq. (12). The factor λ can be estimated in several ways: 1) from the observed Λ/p ratio at AGS energies ($\lambda \approx 1/10$); 2) from the measured[41] probability ratio $P(s\bar{s})/P(u\bar{u})$ in a variety of leptonic and hadronic collisions ($\lambda \simeq 0.1 - 0.15$); 3) from the assumption of thermal and chemical equilibrium of strange particles

$$\lambda \approx (N_{K^-}/N_{K^+})^{1/2} \, e^{-(m_\Lambda - m_N)/T} \approx \frac{1}{7} \tag{13}$$

All of these estimates lead us to the approximate value $\lambda \approx 1/10$, which we adopt here. Extrapolating the observed[39] ratio $N_\alpha/N_p \approx 5 \times 10^{-3}$ (Ne+Pb at 2 GeV/A), we estimate $N_\alpha/N_p \approx 2 \times 10^{-3}$ or $N_\alpha \approx 1/4$ for Au+Au collisions at the AGS. Our rough guess is then

$$N(A,S) \approx \frac{1}{4} P^{A-4} \lambda^{|S|} \approx \frac{1}{4} 10^{4-A-|S|} \tag{14}$$

An experiment with sensitivity $\epsilon = 2.5 \times 10^{-n}$ could detect fragments with

$$|S| + A \leq 3 + n \tag{15}$$

with $n = 11$ for the E864 experiment. Eq. (15) illustrates the importance of high sensitivity; a change of one order of magnitude in ϵ shrinks the accessible domain in $|S| + A$ by one unit. The region of Eq. (15) is enlarged somewhat if one considers NN collisions which produce more than one $s\bar{s}$ pair (the thresholds for $NN \to \Xi KKN$ and $NN \to \Omega^- KKKN$ are at $s^{1/2} = 3.25$ and 4.1 GeV, respectively). With the guess $N(\Xi)/N(\Lambda) \approx \lambda/10 \approx 10^{-2}$ (the additional 1/10 from the restricted phase space for the Ξ), we arrive at the region of sensitivity for E864 shown in Fig. 5.

Strangelets are predicted to lie near the line $S + A = 0$ in Fig. 5, so one should be able to see such objects with up to seven units of strangeness. It is not clear if such relatively light strangelets are bound; Farhi and Jaffe[18] argue that systems with $A \leq 6$ are unbound, on the basis of explicit calculations in the quark shell model. Note that E864 will also be able to find stable dibaryon states with high strangeness $|S| \leq 5$, if such composites exist[19].

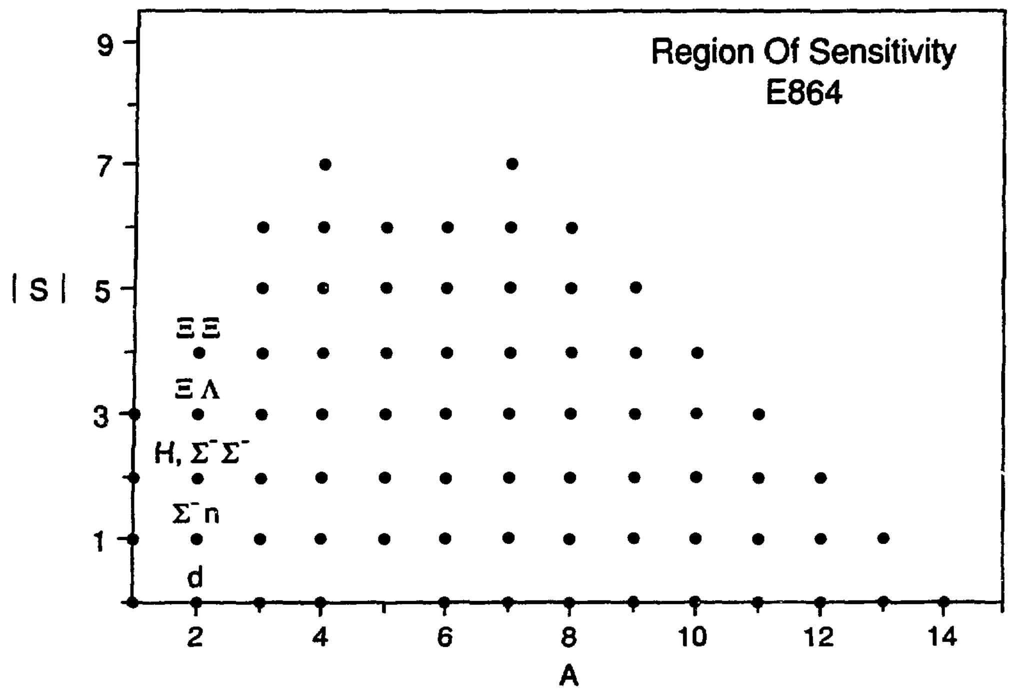

Figure 5: Region of sensitivity of experiment E864 in the (S, A) plane, based on simple coalescence estimates for the production rate of multi–strange clusters.

The strangelets are predicted[18,30] to be of higher density than ordinary nuclei, perhaps 1.5–2 ρ_0. Our coalescence estimates are normalized to the α which has a central density (in a very small volume) comparable to that of a strangelet. Thus we hope that wave function overlaps for a strangelet are not much smaller than we have estimated. Since we have included no explicit dependence of coalescence factors on the binding energy, our estimates might be taken to apply to formation rates for ordinary multi–Λ hypernuclei as well.

The question of the stability of multi–strange composite objects is of fundamental importance in both nuclear and particle physics. A strong theoretical and experimental effort to explore the flavor physics of many–body systems represents a very high priority, and an excellent example of the "intersections" of the two fields.

6. OUTLOOK

There are many exciting prospects for advances in the field of strange particle nuclear physics. The CEBAF and proposed PILAC facilities, providing intense γ and π beams, offer an entry point into the domain of high resolution $S = -1$ hypernuclear spectroscopy. Construction of a KAON factory, with intense K^- beams, would enable great strides to be made in exploring both

$S = -1$ and $S = -2$ systems, qualitatively expanding our very limited knowledge of the latter. For the production of $S \leq -3$ objects, the study of relativistic heavy ion collisions is the most promising method, providing a fighting chance to find stable strange quark droplets or other exotic composites, if they exist.

REFERENCES

1. R.E. Chrien and C.B. Dover, Ann. Rev. Nucl. Part. Sci. 39, 113 (1989).
2. C.B. Dover and D.J. Millener, BNL-44651 (1990), to appear in *Modern Topics in Electron Scattering*, Eds. B. Frois and I. Sick, World Scientific, Singapore (1991).
3. P.H. Pile *et al.*, Phys. Rev. Lett. 66, 2585 (1991).
4. D.J. Millener, C.B. Dover and A. Gal, Phys. Rev. C38, 2700 (1988).
5. D.J. Millener, private communication.
6. W. Brückner *et al.*, Phys. Lett. B79, 157 (1978); R. Bertini *et al.*, Nucl. Phys. A360, 415 (1981).
7. D.J. Millener, A. Gal, C.B. Dover and R.H. Dalitz, Phys. Rev. C31, 499 (1985).
8. D.J. Millener, C.B. Dover and A. Gal, Phys. Rev. C38, 2700 (1988); Y. Yamamoto, H. Bandō, and J. Žofka, Prog. Theor. Phys. 80, 757 (1988).
9. C.B. Dover and A. Gal, Prog. in Particle and Nucl. Phys. 12, 171, Ed. D.H. Wilkinson, Pergamon Press, New York (1984).
10. J.W. Negele and D. Vautherin, Phys. Rev. C5, 1472 (1972).
11. E.H. Auerbach *et al.*, Ann. Phys. (NY) 148, 381 (1983).
12. M. May *et al.*, Phys. Rev. Lett. 51, 2085 (1983).
13. H.A. Thiessen, contribution to these Proceedings, and *Status of PILAC*, in Proc. of the LAMPF Workshop on (π, K) Physics, AIP Conf. Proc. No. 224, Part. and Fields Series 43, Eds. B.F. Gibson *et al.*, (NY) (1991), p. 49.
14. J. Cohen, Intern. J. of Mod. Phys. A4, 1 (1989).
15. M. Bedjidian *et al.*, Phys. Lett. B83, 252 (1980).
16. C.B. Dover and A. Gal, Ann. Phys. 146, 309 (1983).
17. R.L. Jaffe, Phys. Rev. Lett. 38, 195, 617E (1977).
18. E. Witten, Phys. Rev. D30, 272 (1984); E. Farhi and R.L. Jaffe, Phys. Rev. D30, 2379 (1984) and D32, 2452 (1985).
19. V.B. Kopeliovich, B. Schwesinger and B.E. Stern, Phys. Lett. B242, 145 (1990).
20. C.B. Dover and H. Feshbach, Ann. Phys. 198, 321 (1990).
21. M. Danysz *et al.*, Nucl. Phys. 49, 121 (1963); J. Prowse, Phys. Rev. Lett. 17, 782 (1966).
22. R.H. Dalitz *et al.*, Proc. Royal Soc. London A426, 1, (1989).

23. S. Aoki *et al.*, preprints DPNU–91–06 and DPNU–91–07, Nagoya Univ. (1991).
24. C.B. Dover, D.J. Millener, A. Gal and D.H. Davis, submitted to Phys. Rev. C (1991).
25. M. Oka, K. Shimizu and K. Yazaki, Nucl. Phys. A464, 700 (1987).
26. D. Zhu, C.B. Dover, A. Gal and M. May, BNL–46135, submitted to Phys. Rev. Lett. (1991).
27. G.B. Franklin, Nucl. Phys. A450, 117c (1986).
28. P. Barnes, Nucl. Phys. A478, 127c (1988) and A479, 89c (1988).
29. M. Rufa *et al.*, Phys. Rev. C42, 2469 (1990).
30. M.S. Berger and R.L. Jaffe, Phys. Rev. C35, 213 (1987). To connect with the notation of this paper: $a_V = m_N - \epsilon_0$, $a_S = 4\pi\sigma r_0^2$, $a_C = 3\alpha/5r_0$.
31. W.S.C. Williams, *Nuclear and Particle Physics*, Clarendon Press, Oxford (1991), see pp. 54–65.
32. In Eq. (9), we have used the corrected value for the surface tension σ given by Berger and Jaffe (erratum to Phys. Rev. C).
33. O. Hansen, Comments Nucl. Part. Phys. 20, 1 (1991).
34. J. Barrette *et al.*, Phys. Lett. B252, 550 (1990).
35. E864: Production of Rare Composite Objects in Relativistic Heavy Ion Collisions, a Brookhaven, U. Massachusetts, MIT, McGill, U. New Mexico, Penn State, Yale collaboration (J. Sandweiss and R.D. Majka, spokespersons).
36. H.J. Crawford, private communication of E858 preliminary results; see also E878: Investigation of Antinucleus Production and Search for New Particles in Nucleus–Nucleus Collisions at the AGS (H. Crawford, spokesperson).
37. C. Greiner, D.H. Rischke, H. Stöcker and P. Koch, Phys. Rev. D38, 2797 (1988); C. Greiner and H. Stöcker, preprint (1991).
38. J. Kapusta, Phys. Rev. C21, 1301 (1980).
39. S. Nagamiya *et al.*, Phys. Rev. C24, 971 (1981).
40. A.Z. Mekjian, Phys. Rep. C17, 1051 (1978).
41. J.L. Bailly *et al.*, Phys. Lett. B195, 609 (1987).